ELSEVIER

Sedimentary Geology 136 (2000) 71–88

Sedimentary Geology

www.elsevier.nl/locate/sedgeo

Duration of deposition from decelerating high-density turbidity currents

J.H. Baas[a,*], R.L. van Dam[b], J.E.A. Storms[c]

[a]*School of Earth Sciences, University of Leeds, LS2 9JT Leeds, UK*
[b]*Faculty of Earth Sciences, Vrije Universiteit, De Boelelaan 1085, 1081HV Amsterdam, Netherlands*
[c]*Department of Applied Earth Sciences, Delft University of Technology, P.O. Box 5028, 2600 GA Delft, Netherlands*

Received 24 September 1999; accepted 23 March 2000

Abstract

Using recent advances in the stability analysis of current ripples, a new model for the calculation of duration of sediment deposition from decelerating high-density turbidity currents is proposed. The model, named TDURE, refines a duration model proposed by Allen (1991) (J. Sediment. Petrol. 61, 291–295) by calculating the accumulation time of the rippled T_c-division separately from the massive and plane parallel-laminated T_{ab}-divisions in Bouma-type turbidites. TDURE consists of three modules. In the first module, the accumulation time for the T_a- and T_b-divisions is approximated by assuming a linear decrease in sedimentation rate with height in the turbidite. As in the original model, a straight line is fitted through inferred sedimentation rates at the T_{ab}- and T_{bc}-boundaries. In the second module, angle of climb of ripples, thickness of the T_c-division and grain size distribution are used in empirical relationships between ripple migration rate and a grain-related mobility parameter to estimate the accumulation time of the T_c-division. In the third module, the expected development of ripple size across the T_c-division is calculated using empirical relationships between rate of development of ripple height and grain-related mobility parameter, and subsequently compared with the observed development of ripple size in the turbidite. In this way, the accuracy of the accumulation time calculated in module 2 can be verified independently. TDURE was tested using Bouma-type turbidites from the Doheny Channel (Capistrano Fm., CA, USA) and the Flysch di Motta (Calabria, Italy). Accumulation times of 12 and 10.75 min for the T_c-division, and 19 and 16 min for the T_{abc}-sequence were calculated for the Doheny Channel and the Flysch di Motta turbidites, respectively. Although module 3 underestimates the rate of development of current ripples near the T_{bc}-boundary in both beds, ripple size at the T_{cd}-boundary is calculated accurately. The underestimation of development rate may be caused by differences between flow conditions in experimental flumes on which the model calculations are based and turbidity-current dynamics.

Keywords: turbidity current; numerical model; accumulation time; current ripples

1. Introduction

The composite sequence of sedimentary structures in turbidite beds, known as the Bouma-sequence (Bouma, 1962), is the product of gradual waning of a turbidity current over a depositional site (Kuenen and Migliorini, 1950; Kuenen, 1953; Lowe, 1982). Each level within a turbidite records the complex interaction between the strength of the current, the concentration of moving sediment, its size distribution and composition, and the configuration of the

* Corresponding author. Tel.: +44-113-223-6624; fax: +44-113-233-5259.
E-mail address: j.baas@earth.leeds.ac.uk (J.H. Baas).

0037-0738/00/$ - see front matter
PII: S0037-0738(00)00088-9

underlying bed surface at the time of deposition. In spite of these complex interrelationships, the complete Bouma-sequence, T_{abcde}, and most of its incomplete varieties, can be predicted from theoretical paths of decelerating flow in bedform stability diagrams (Allen, 1984). This offers the possibility to reconstruct the dynamics of turbidity currents from the type of sedimentary structures and vertical grain-size trends in their deposits (Komar, 1985; Hiscott, 1994). Such knowledge helps in the understanding and prediction of depositional mechanisms of turbidity currents, which in turn is important for the sedimentological explanation of the dispersal of sediment in deep-marine environments.

Another important aspect of this type of research is the timing of deposition, as it is closely related to the velocity gradient within a turbidity current and thus to the efficiency of downslope transport of sediment. Allen (1991) proposed a simple model to estimate the duration of a turbidity current, based on an experimentally derived sedimentation rate for the suppression of plane-parallel lamination (Arnott and Hand, 1989) and theoretical sedimentation rates at the T_{bc}-boundary (Allen, 1971a). The present paper extends Allen's model by separately calculating the accumulation time of the T_c-division in Bouma-type turbidites. A new model, named TDURE, is proposed based on recent advances in the stability analysis of current ripples (Alexander, 1980; Tsujimoto and Nakagawa, 1982; Lam Lau, 1985; Raudkivi and Witte, 1990; Coleman, 1991; Kühlborn, 1993; Baas, 1994; Oost and Baas, 1994; Baas and de Koning, 1995; Raudkivi, 1997; Baas, 1999; Storms et al., 1999). These studies provide fundamental relationships between ripple morphology, migration rate and development time, current strength and grain size, that allow estimation of the accumulation time of the T_c-division to be approached in two ways. The first and principal method uses ripple migration rate to calculate the time needed to form a T_c-division of given thickness and angle of climb of ripple trains. The second method is based on the expected development of ripple height on a flat bed, and is used to verify the results obtained with the principal method. Examples of duration calculations with TDURE are discussed for a T_{abcde}-bed from the Doheny Channel turbidite in the Capistrano Formation, Mio-Pliocene, CA (Piper and Normark, 1971; Komar, 1985; Allen, 1991; Hiscott, 1994) and for a T_{abcd}-bed from the Flysch di Motta (Miocene) of southern Italy.

2. Theoretical background

Komar (1985) was one of the first authors who proposed a model based on flow-competence concepts to calculate bed shear stresses from grain sizes at various heights along a turbidite profile. In his calculations, flow competence was represented by the ratio between settling velocity of a characteristic particle and bed shear velocity. Deposition was presumed to occur only when the ratio is larger than unity (suspension criterion: Bagnold, 1966; Middleton, 1976). Hence, flow competence can be described as a measure for the maximum particle size carried in suspension by a turbidity current of given hydraulic strength (cf. Hiscott and Middleton, 1979; van Tassell, 1981; Bowen et al., 1984; Piper et al., 1988). Komar (1985) computed a bed shear stress profile for the Doheny Channel turbidite (Piper and Normark, 1971), but with limited success. The bed shear stress derived from the suspension criterion at the plane parallel-laminated T_b- to rippled T_c-transition was significantly lower than the bed shear stress at the corresponding phase boundary in Allen's bedform stability diagrams (Allen, 1984).

Hiscott (1994) addressed this problem by assuming that not the loss of competence, but the loss of capacity is the fundamental process controlling deposition from turbidity currents. The capacity concept dictates that a current of given hydraulic strength has a maximum volume of particles it can carry in suspension. During flow deceleration, the capacity progressively decreases, and particles of different size, as opposed to single-size particles in Komar's (1985) model, collectively settle onto the sediment bed. Using a Rouse-type relationship between volume of suspended sediment and current strength (Rouse, 1937), Hiscott (1994) was able to improve the correspondence between theory and data for the Doheny Channel turbidite. It thus appears that the capacity concept is preferable over the competence concept in analysing sediment deposition from the body of waning turbidity currents. This was already suggested in an earlier paper by Allen (1991), in which the "overloaded nature" of collapsing turbidity currents was used to

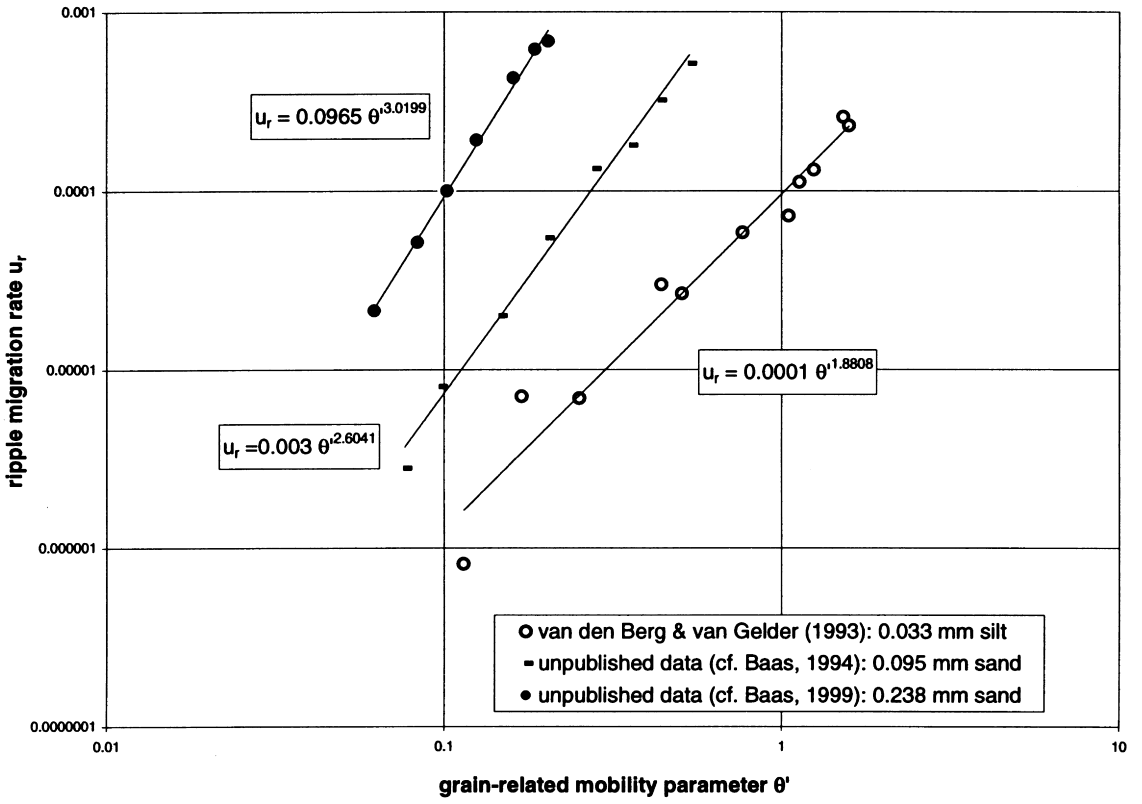

Fig. 1. Empirical relationships between the migration rate of equilibrium current ripples and the grain-related mobility parameter for different grain sizes. The equations denote best-fit power functions, corresponding with the straight lines through the data points. In 0.095 and 0.238 mm sand, migration rates are average values, based on several hundreds of measurements.

explain the suppression of plane-parallel lamination below the T_{ab}-transition. Similar assumptions will be made in the present study.

A principal step in the hydrodynamic analysis of structural divisions in turbidites is to delimit the flow conditions of the corresponding bedform phases from bedform stability diagrams. Bedform stability diagrams define the existence boundaries of various types of bedform as a function of grain size and current energy in unidirectional laboratory currents (Allen, 1984; Southard and Boguchwal, 1990; van den Berg and van Gelder, 1993). Bedform type and grain size can be determined in most sedimentary deposits. Consequently, flow conditions at the time of deposition, usually expressed by velocity (Southard and Boguchwal, 1990) or (non-dimensionalised) shear stress (Allen, 1984), can be estimated directly from bedform stability diagrams. For example, Allen (1984) depicted flow paths of hypothetical turbidity currents in bedform stability diagrams to explain in hydrodynamic terms the structural (Bouma-type) sequences observed in turbidites. A quantitative reconstruction of flow conditions, however, is complicated by the overlap of stability regions of bedform phases present in those stability diagrams that use flow parameters strongly related to bedform roughness or energy slope (Allen, 1984; see discussion by van den Berg and van Gelder, 1993). Such parameters include flow power and Shields or mobility parameter. Van den Berg and Van Gelder, (1993) proposed a modified bedform stability diagram, in which a better separation of bed configurations was achieved by plotting a grain-related mobility parameter θ', based on grain roughness instead of form roughness, against the non-dimensional grain

parameter D_*. The corresponding equations are:

$$\theta' = \frac{U^2}{(\rho_s/\rho - 1)C'^2 D_{50}} \quad (1)$$

$$D_* = \left(\frac{(\rho_s/\rho - 1)g}{\nu^2}\right)^{1/3} D_{50} \quad (2)$$

where U is the mean current velocity, ρ_s is the sediment density, ρ is the density of water, D_{50} is the median grain size, ν is the dynamic viscosity, and C' is the grain-related Chézy coefficient with the Nikuradse roughness parameter k_s equal to three times the 90-percentile of the grain-size distribution (van Rijn, 1990). The potential value of the modified stability diagram for paleohydraulic reconstruction was further illustrated by its successful application to natural river flows (van den Berg and van Gelder, 1993: their Fig. 6). We will use θ'-values at the boundaries of the current-ripple regime in van den Berg and van Gelder's (1993) bedform stability diagram as hydraulic limits for duration calculation of turbidity currents.

Empirical relationships between ripple migration rate and grain-related mobility parameter, and between ripple development stage and grain-related mobility parameter are the backbone of the model proposed here. These relationships are derived from the literature records on current ripple dynamics. The dependence of the migration rate of equilibrium ripples on current energy can be approximated by a power function of the general form:

$$u_r = a\theta'^b \quad (3)$$

where u_r is the ripple migration rate, recalculated to an equivalent water temperature of 10°C (cf. Southard and Boguchwal, 1990). The coefficients a and b are grain-size dependent. Best-fit power functions for silt (van den Berg and van Gelder, 1993), very fine sand (Baas, 1994) and fine sand (Baas, 1999) are given in Fig. 1.

Current ripples developing on a flat bed, such as at the T_{bc}-boundary in turbidites, evolve through various development stages towards a linguoid equilibrium morphology with constant height and length (Baas, 1994, 1999). The rate of development is a function of current strength and grain size. For the development of ripple height from flat bed conditions in unsteady flow, the relationship can be expressed as (Oost and Baas, 1994):

$$\frac{H(t)}{H_E} = 1 - (0.01)^{S_H} \text{ and } S_H = \int_0^t \frac{dt}{\tau_E(t)} \quad (4)$$

where $H(t)$ is the ripple height at time t, H_E is the equilibrium ripple height (constant for a given grain size), S_H is the development stage of ripple height, and $\tau_E(t)$ is the equilibrium time, i.e. the time needed to reach equilibrium ripple height at the instantaneous current strength at time t. The development stage is equal to zero for a flat bed, and one or higher for equilibrium conditions. A similar equation has been proposed for the development of ripple length (Oost and Baas, 1994). Equilibrium time $\tau_E(t)$ changes with gradient in current energy and grain size as follows:

$$\tau_E = \left(\frac{\theta' - \theta'_{crit}}{c}\right)^{-1/d} \quad (5)$$

where c and d represent grain-size dependent coefficients, θ'_{crit} represents the critical mobility (Shields) parameter for particle entrainment at the given grain size, and τ_E is given in hours. For well-sorted, very fine quartz sand ($D_{50} = 0.095$ mm; cf. Baas, 1994) $\theta'crit = 0.075$, $c = 0.198$ and $d = -0.697$. For well-sorted, fine quartz sand ($D_{50} = 0.238$ mm; cf. Baas, 1999) $\theta'_{crit} = 0.046$, $c = 0.106$ and $d = -0.456$. Similar equations have been proposed for the development of ripple length (Baas, 1994, 1999; Oost and Baas, 1994).

3. Model

TDURE is a mathematical model that calculates the duration of deposition of decelerating high-density turbidity currents from their deposits. It should be noted that the term *high-density turbidity current* used throughout this paper follows the definition of Lowe (1982), thus applying the term to all beds containing a non-tractional division at their base, and not restricting its use to massive, "structureless" beds. TDURE is an extension of a model proposed by Allen (1991). Allen (1991) introduced a procedure to estimate the duration of a turbidity current from the rate of sediment deposition at the T_{ab}- and T_{bc}-transitions. From a linear fit through these points, a duration of 20–52 min was derived for the turbidity current,

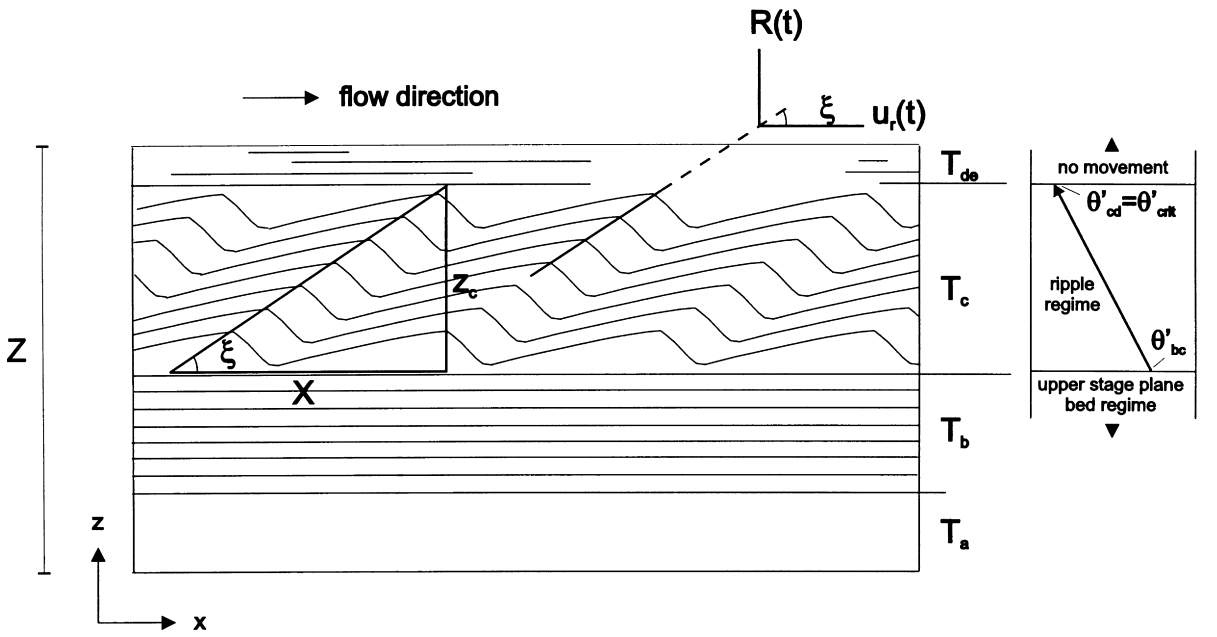

Fig. 2. Schematic drawing of a turbidite bed with physical parameters as used in the model calculations. See text for explanation of symbols.

which formed the turbidite in the Doheny Channel (Piper and Normark, 1971; Komar, 1985). In TDURE, we calculate the accumulation time for the T_c-division separately from that of T_a- and T_b-divisions. TDURE consists of three computational modules: module 1 calculates the accumulation time of the T_{ab}-divisions; module 2 uses temporal changes in ripple migration rate to determine the accumulation time of the T_c-division; and module 3 uses bedform dynamics to verify the calculations done with module 2. In the present form, application of TDURE is confined to T_{abc}-type beds. The model does not account for sediment accumulation in T_d- and T_e-divisions, hence it restricts the duration calculations to the basal non-tractional and subsequent tractional depositional stages. It is assumed that these fine-grained intervals are the result merely of settling from suspension without traction, formed after passage of the main body of the turbidity current. This may be an oversimplification, however, because traction may induce the faint parallel lamination in T_d-divisions (Stow and Bowen, 1978, 1980), and thus the top of the T_c-division need not be the level of transition from the body to the wake of a turbidity current, as discussed by Allen (1991). The accumulation times given by TDURE correspond to the lower duration estimates in Allen's (1991) model.

3.1. Module 1: calculation of accumulation time for T_a- and T_b-divisions

Module 1 determines the accumulation time of the T_a- and T_b-divisions, τ_a and τ_b, using the integral function of Allen (1991), but with different limits:

$$\tau_a = \int_0^{z_{ab}} \frac{dz}{R(z)} \tag{6}$$

$$\tau_b = \int_{z_{ab}}^{z_{bc}} \frac{dz}{R(z)} \tag{7}$$

where z_{ab} and z_{bc} denote the height of the T_{ab}-boundary and the T_{bc}-boundary, respectively. $R(z)$ is approximated by a straight line defined by points (z_{ab},R_{ab}) and (z_{bc},R_{bc}) along the bed profile, as in the original model (Allen, 1991). The sedimentation rate at the T_{ab}-boundary, $R_{ab} = 6.7 \times 10^{-4}\ \mathrm{ms}^{-1}$, was taken from Arnott and Hand's (1989) study on the suppression of plane-parallel lamination in high-concentration laboratory currents. The sedimentation rate at

the T_{bc}-boundary, R_{bc}, was calculated using the following equation (Allen, 1971a):

$$R_{bc} = 9.386 \frac{D_{bc}^{1.5} \tan \xi}{H_{bc}} \quad (8)$$

where D_{bc} is the mean grain size at the T_{bc}-boundary, ξ is the angle of climb of ripples forming just above the boundary, and H_{bc} is the characteristic height of the ripples.

3.2. Module 2: calculation of accumulation time for T_c-division

The second module of TDURE calculates the duration of deposition of the T_c-division. The sedimentological parameters used in these calculations include the angle of climb ξ of current ripples, the ripple migration rate $u_r(t)$, the sedimentation rate $R(t)$, the total horizontal displacement of ripples across the T_c-division X, the thickness of the T_c-division z_c and the gradient in grain-related mobility parameter $\theta'_{cd} - \theta'_{bc}$ (Fig. 2). The total horizontal displacement of a train of ripples in the T_c-division is expressed geometrically by:

$$X = \frac{z_c}{\tan \xi} \quad (9)$$

or in terms of sedimentation rate and ripple migration rate:

$$u_r(t) = \frac{R(t)}{\tan \xi} \quad (10)$$

This equation, combined with an u_r–θ'-function for the appropriate grain size (Fig. 1), can be used as alternative to Eq. (8) (Allen, 1991) to calculate R_{bc}. Comparative examples will be given when testing TDURE for natural turbidites (see below). In order to simplify calculations, it is assumed that ripples in the T_c-division climb at a constant angle. Along-bed variations in angle of climb smaller than ^ 5° can be ironed out by using an average angle of climb in the model calculations. Variations larger than 5°, however, require that temporal changes in angle of climb be incorporated into TDURE. The use of an average angle of climb, as in the present model, will then provide a rough estimate of accumulation time, but will not allow for the accurate simulations of bedform development with module 3.

Current ripples in the T_c-division migrate over a horizontal distance dx during each time step dt. The total horizontal displacement X is:

$$X = \int_0^X \mathrm{d}x \quad (11)$$

which is equal to:

$$X = \int_0^{\tau_c} u_r(t)\, \mathrm{d}t \quad (12)$$

in terms of temporal change in migration rate and accumulation time. Eq. (12) is the basic formula for calculating the duration of deposition of the T_c-division. The total horizontal displacement can be measured directly from the turbidite bed. Alternatively, it can be determined from the average angle of climb and the thickness of the T_c-division through Eq. (9). The accumulation time τ_c can be calculated by solving the integral function, provided that the ripple migration rate is known. Since migration rate changes with current strength and grain size according to the equations given in Fig. 1, Eq. (12) can be rewritten into the general form:

$$X = \int_0^{\tau_c} a\theta'(t)^b \, \mathrm{d}t \quad (13)$$

where coefficients a and b conform to the average grain size in the T_c-division, thus accounting for vertical (normal) size gradients and assuming minor influence of size sorting and other textural and compositional parameters. Strictly speaking, Eq. (13) is only applicable to linguoid equilibrium ripples, i.e. the type of ripples for which Eq. (3) is valid. It is to be expected, however, that initial, small ripples developing on the flat T_{bc}-boundary will migrate faster than larger ripples at equivalent flow conditions, leading to overestimation of accumulation time in the model. Yet, the decrease in migration velocity is relatively small (Baas, unpublished data) and limited in time, as the high velocities at the T_{bc}-boundary involve a rapid increase of ripple size during the initial stages of ripple development (cf. Eqs. (4) and (5)). A further assumption in the model is that the settling of sediment from suspension has a negligible retarding or accelerating effect on ripple migration rate. This effectively means that the excess sediment is used entirely for vertical aggradation, and thus is distributed evenly over the rippled sediment surface. Also, the effect of settling lags on the timing

of deposition of fine-grained sediment, particularly near the top of the T_c-division, is considered to be small.

A relationship between grain-related mobility parameter and time is required to solve the integral in Eq. (13) and calculate the accumulation time for the T_c-division. Simple single-surge-type turbidity currents are characterised by a rapid increase in current velocity during passage of the head and a more gradual exponential ("concave upward") decrease thereafter (e.g. Kneller et al., 1997). Simpson (1997) referred to an exponent of 1/3 for the self-similar flow regime of experimental shallow-water density currents, but it is questionable whether this value can be applied to natural sediment-laden currents. Module 2 of TDURE approximates the part of the velocity profile in which ripples are formed by a linear decrease in grain-related mobility parameter (Fig. 2):

$$\theta'(t) = \theta'_{bc} + \frac{\theta'_{cd} - \theta'_{bc}}{\tau_c} t \qquad (14)$$

The validity of this function can be checked with an independent method based on the expected development of ripple dimensions in the T_c-division. This method is part of module 3, and will be described in the following section. In Eq. (14), θ'_{bc} represents the θ'-value at the upper limit of the current ripple regime in the bedform stability diagram of van den Berg and van Gelder (1993). The required D_*-value at the T_{bc}-boundary is given by Eq. (2). This equation contains the dynamic fluid viscosity, which is primarily dependent on water temperature. In all but a few cases, the temperature will be unknown. TDURE uses a standard temperature of 10°, which is equivalent to $\nu = 1.307 \times 10^{-6}\ m^2\ s^{-1}$. In most deep-marine environment θ'_{bc}-values can be determined directly from the stability diagram or calculated using the following set of best-fit equations:

$$\begin{aligned}
\theta'_{bc} &= 1.36 && \text{for } D_* \le 0.84 \\
\theta'_{bc} &= 1.29 D_*^{-0.3} && \text{for } 0.84 < D_* \le 2.16 \\
\theta'_{bc} &= 2.16 D_*^{-0.97} && \text{for } 2.16 < D_* \le 3.04 \\
\theta'_{bc} &= 2.06 \times 10^7 D_*^{-15.44} && \text{for } 3.04 < D_* \le 3.20 \\
\theta'_{bc} &= 2.24 D_*^{-1.65} && \text{for } 3.20 < D_* \le 4.09 \\
\theta'_{bc} &= 0.43 D_*^{-0.49} && \text{for } 4.09 < D_* \le 6.99
\end{aligned} \qquad (15)$$

In these equations, it is assumed that the accumulation time is too short to form dunes for $D_* > 3.04$ (cf. Allen, 1984).

Following the earlier assumption that tractional transport is absent above the T_{cd}-boundary, θ'_{cd} is equivalent to the critical mobility parameter for particle entrainment θ'_{crit} given by (Miller et al., 1977; van Rijn, 1993):

$$\theta'_{crit} = 0.11 D_*^{-0.54} \qquad \text{for } D_* \le 10 \qquad (16)$$

Inserting Eq. (14) into Eq. (13) and solving the integral function yields the following equation for the accumulation time of the T_c-division:

$$\tau_c = \frac{X(b+1)(\theta'_{cd} - \theta'_{bc})}{a(\theta'^{\,b+1}_{cd} - \theta'^{\,b+1}_{bc})} \qquad (17)$$

The total duration of deposition for the T_{abc}-bed, τ_{abc}, can now be determined by simple addition of the accumulation times provided by modules 1 and 2.

3.3. Module 3: verification of linear θ'–t-function

The accuracy of the linear relationship between grain-related mobility parameter and time proposed in module 2 can be checked by comparing the expected development of ripple size across the T_c-division with the visible change in ripple size in the turbidite studied. In the present paper, we will base this comparison on ripple height, though a similar analysis can be done for ripple length. The theoretical development of ripple height in unsteady flow over very fine and fine sand is given by Eqs. (4) and (5). The equations were derived from experiments at non-aggrading conditions, so the effect of suspended sediment concentration on ripple development should be considered before application in module 3. When discussing relationships between ripple migration rate and current strength above, it was assumed that sediment settling from suspension is distributed evenly over the sediment surface. If so, the excess sediment is used only to increase bed thickness, and consequently migration rate and ripple dimensions should not be different from the non-aggrading situation. Previous studies seem to justify the independence of ripple size on sedimentation rate. Allen (1973) conducted flume experiments in the current ripple regime at aggrading and non-aggrading conditions. His records do not show a consistent change in

ripple size with the introduction of excess sediment. In some runs, an increase in suspended sediment fallout matched an increase in mean ripple height by up to 3 mm, in others, the height decreased by several mm. This agrees well with the results of detailed flume experiments by Ashley et al. (1982). They observed that "ripples seemed to show about as much variability in geometry and migration rate during the runs, while conditions of flow and aggradation were changing, as during equilibrium migration of ripples in the absence of sediment feed". Ripples attained a slightly more rounded profile at high suspended-load fallout rate in studies by Jopling and Walker (1968) and Allen (1971b), but their size remained virtually constant. Arnott and Hand (1989) simulated conditions prevailing during deposition of T_c-divisions in a flume, and found no significant difference in size with ripples in non-aggrading runs. The same conclusion can be drawn from ripple height data presented by Storms et al. (1999), although their sedimentation rates were an order of magnitude smaller than in Arnott and Hand's (1989) experiments. Walker (1969) found an upward decrease in ripple height in turbidites of the Cloridorme Fm. of Quebec, Canada, but the data presented in his Table 1 showed no apparent relationship between ripple height and mean angle of climb. The above observations inspire confidence to extend the use of Eqs. (4) and (5) to T_c-divisions, in which high suspended-sediment fallout rates are the rule rather than the exception.

Eqs. (4) and (5) are combined to give the following equation for the cumulative development of ripple height in turbidites:

$$\frac{H(t)}{H_E} = 1 - (0.01)^{S_H} \quad \text{and} \quad S_H = c^{-1/d} \int_0^t [\theta'(t) - \theta'_{cd}]^{1/d}\, dt \tag{18}$$

where $\theta'_{cd} = \theta'_{crit}$ according to Eq. (16), $t \leq \tau_c$, and c and d represent the grain-size dependent coefficients in Eq. (5). At present, relationships between current strength and equilibrium time are available for 0.095 mm sand and 0.238 mm sand only. In TDURE, the coefficients corresponding to one of these sands are selected based on the average grain size in the T_c-division of the studied turbidite. The equilibrium height H_E is estimated from the z_c-averaged grain size $\bar{D}_{50}$, using a linear interpolation between known equilibrium heights of 13.1 mm and 17.0 mm for 0.095 mm and 0.238 mm sand, respectively (Baas, 1994, 1999). All grain sizes are converted to ϕ-scale before interpolation.

Using the same linear relationship between mobility parameter and time as in module 2 (Eq. (14)), and assuming that the accumulation time calculated in module 2 is correct, the following general solution for the integral in Eq. (18) is derived:

$$S_H = \left(\frac{\theta'_{bc} - \theta'_{cd}}{c\tau_c} \right)^{1/d} \frac{(\tau_c^{1+(1/d)} - (\tau_c - t)^{1+(1/d)})}{1 + \frac{1}{d}} \tag{19}$$

which collapses to:

$$S_H = \frac{\tau_c(\theta'_{bc} - \theta'_{cd})^{1/d}}{c^{1/d}\left(1 + \frac{1}{d}\right)} \tag{20}$$

for the final ripple height at the top of the T_c-division ($t = \tau_c$). Eq. (19) is used to depict the temporal development of ripple height in a H–t-plot. However, for comparison with actual development of ripple height, a H–z-plot is more useful. The relation between the temporal domain and the spatial domain is given by the following integral:

$$\int_0^z dz = \tan\xi \int_0^t a\theta'(t)^b\, dt \tag{21}$$

which is essentially a more general version of Eq. (13) combined with Eq. (9). In Eq. (21), z represents the instantaneous height at time t during bed aggradation. The solution of this equation is:

$$z = \frac{a\tan\xi}{1+b}\left[\left(t + \frac{\theta'_{bc}}{\Theta} \right)(\theta'_{bc} + \Theta t)^b - \frac{\theta'^{\,1+b}_{bc}}{\Theta} \right] \tag{22}$$

where Θ is the gradient of the θ'–t-profile equal to $(\theta'_{cd} - \theta'_{bc})/\tau_c$. With this equation, time is converted to height along bed, thus allowing a theoretical H–z-plot to be constructed. The theoretical trend in ripple height is then compared with the observed trend across the T_c-division to verify the chosen mobility parameter profile.

Local sedimentation rates during build-up of the T_c-division are calculated via Eq. (21) by setting the limits of integration to $\Delta z = z_2 - z_1$ and $\Delta t = t_2 - t_1$, and subsequently determining the ratio of these values.

Table 1
Results of duration calculations for the Doheny Channel turbidite and bed FM11 from the Flysch di Motta

	Doheny Channel	Flysch di Motta
Input parameters		
Thickness of T_a-division (cm)	3	33
Thickness of T_b-division (cm)	17	5
Thickness of T_c-division (cm)	7	5
Thickness of $T_{d(e)}$-divisions (cm)	^ 5	2
Total bed thickness	32	45
Median grain size at T_{bc}-boundary (mm)	0.138	0.135
Median grain size at T_{cd}-boundary (mm)	0.096	0.076
Ripple height (mm)	12	12.4 ^ 2.7
Angle of climb of ripples	12°	9° (7°–9°–11°)
Module 1		
Extrapolated sedimentation rate at base (with Eq. (8)) (mm/s)	0.741	3.85
Extrapolated sedimentation rate at base (with Eq. (23)) (mm/s)	0.732	3.45
Sedimentation rate at T_{ab}-boundary (mm/s)	0.670	0.670
Sedimentation rate at T_{bc}-boundary (with Eq. (8)) (mm/s)	0.270	0.188
Sedimentation rate at T_{bc}-boundary (with Eq. (23)) (mm/s)	0.316	0.249
Accumulation time of T_a-division (with Eq. (8)) (min)	0.71	3.02
Accumulation time of T_a-division (with Eq. (23)) (min)	0.71	3.24
Accumulation time of T_b-division (with Eq. (8)) (min)	6.44	2.20
Accumulation time of T_b-division (with Eq. (23)) (min)	6.01	1.96
Module 2		
Total horizontal displacement of ripples (cm)	32.9	31.6
Grain-related mobility parameter at T_{bc}-boundary	0.764	0.780
Grain-related mobility parameter at T_{cd}-boundary	0.075	0.085
Average grain size in T_c-division (mm)	0.115	0.101
Coefficient *a* in Eq. (13)	0.003	0.003
Coefficient *b* in Eq. (13)	2.6041	2.6041
Ripple migration rate at T_{bc}-boundary (mm/s)	1.490	1.570
Accumulation time of T_c-division (min)	12.00	10.75
Total accumulation time (min)	18.72–19.15	15.95–15.97
Module 3		
Cumulative ripple development stage at T_{cd}-boundary	0.491	0.455
Equilibrium ripple height (mm)	13.9	13.4
Calculated ripple height at T_{cd}-boundary (mm)	12.5	11.7

The trends in sedimentation rate are visualised in *R*–*z*- and *R*–*t*-plots.

4. Application

TDURE was tested using two Bouma-type turbidites from the Doheny Channel in the Capistrano Formation (Mio-Pliocene, CA: Piper and Normark, 1971) and the Flysch di Motta (Miocene) in SW Calabria, Italy (Baas et al., 1999; Seim and Baas, 1999), for which detailed grain-size records and current ripple data are available. The computational results are summarised in Table 1.

4.1. Doheny channel

Description—The Capistrano Formation (Mio-Pliocene) in an outcrop near Dana Point in Orange County, CA, consists of a succession of dominantly coarse-grained sandstone and conglomerate,

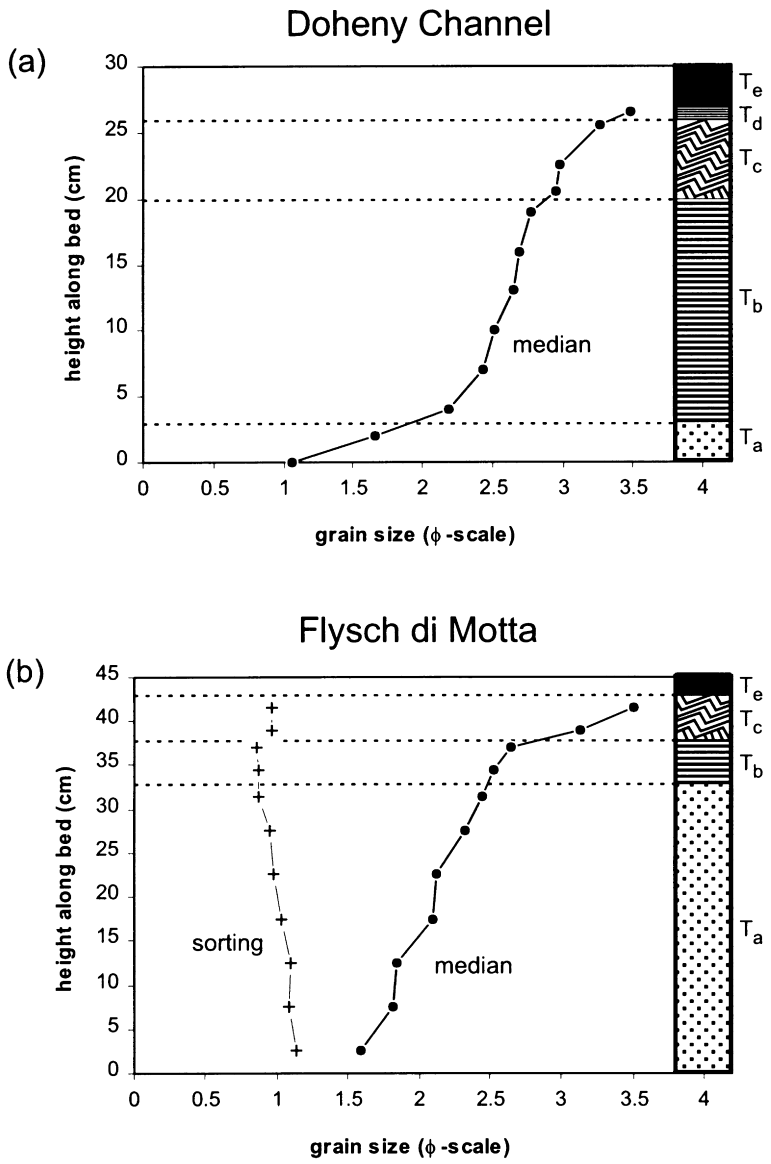

Fig. 3. Vertical trends in median grain size and sorting (Folk, 1968) for: (a) Doheny Channel turbidite; and (b) bed FM11 from the Flysch di Motta. Grain size and sorting are in ϕ-units. The fill patterns in the schematic logs denote Bouma-divisions.

interpreted as a submarine channel fill on a deep-sea fan (Bartow, 1966; Piper and Normark, 1971). An interval with fine-grained, normally graded sandstone beds near the top of the outcrop was inferred to be deposited by turbidity currents still confined to the channel, but with lower energy than the flows, which deposited the coarse-grained sediment below. Komar (1985) studied one such bed in detail with the objective to reconstruct flow conditions during deposition. The turbidite is 30–32 cm thick with an erosive base and a flat top. It consists of a complete Bouma-sequence with a T_a-division ranging in thickness from 1 to 3 cm, the exact value depending on the degree of basal erosion, a 17 cm thick T_b-division, and

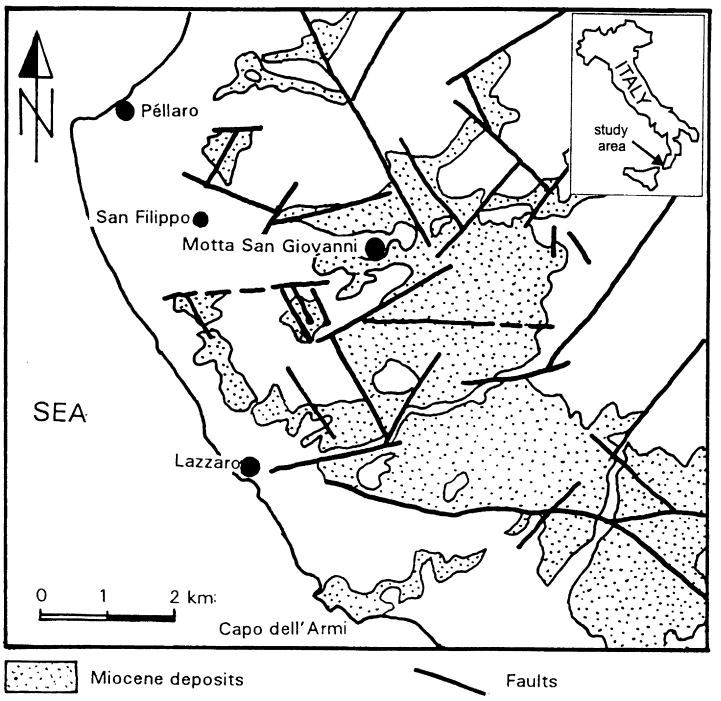

Fig. 4. Sketch map of Flysch di Motta outcrops along the Messina Strait in southern Italy.

a T_c-division with a thickness of 7 cm (Table 1). A T_d-division, 1 cm thick, was identified on top of the rippled interval, and is in turn overlain by an approximately 5 cm thick layer of massive mud, interpreted as a T_e-division (Komar, 1985). The Doheny Channel turbidite is normally graded from medium sand at its base to very fine sand in the T_d-division (Fig. 3a). From Komar's (1985) granulometric data, we determined a median grain size of 0.138 mm at the T_{bc}-boundary, a median grain size of 0.096 mm at the T_{cd}-boundary, and a z_c-averaged grain size of 0.115 mm. Allen (1991) reported a characteristic ripple height of 12 mm, with an angle of climb of 12° near the base of the T_c-division. Yet, from a photograph presented by Komar (1985), it appears that the ripple height is less than 12 mm in the lower 1.5 cm of the bed.

Module 1—Module 1 of TDURE estimates an accumulation time of 0.71 min for the T_a-division and 6.44 min for the T_b-division of the Doheny Channel turbidite. These results are based on Eqs. (6)–(8), hence pursuing the original model of Allen (1991). As an alternative to Eq. (8), the sedimentation rate at the T_{bc}-boundary was also determined by using the following equation (cf. Eq. (10)):

$$R_{bc} = u_{r,bc} \tan \xi \tag{23}$$

The ripple migration rate at the T_{bc}-boundary, $u_{r,bc}$, was derived from Eq. (3), applying coefficients a and b pertinent to 0.095 mm sand (Fig. 1). This grain size is a reasonable approximation for the grain size measured at the T_{bc}-boundary (Table 1). Eq. (23) provides a slightly greater sedimentation rate than Allen's (1991) model, but the accumulation time for the T_a-division is not significantly different. The accumulation time for the T_b-division reduces by slightly less than 30 s (Table 1).

Module 2—In the module 2 calculations, we applied coefficients a and b pertinent to 0.095 mm sand (Eq. (3); Fig. 1). It was assumed that the basal angle of climb of 12° (Allen, 1991) applies to the entire T_c-division. However, the true angle of climb may have decreased further upwards in the T_c-division, where Komar (1985) found no clear indication of climbing ripples. The degree to which this affects duration calculations will be addressed in more detail

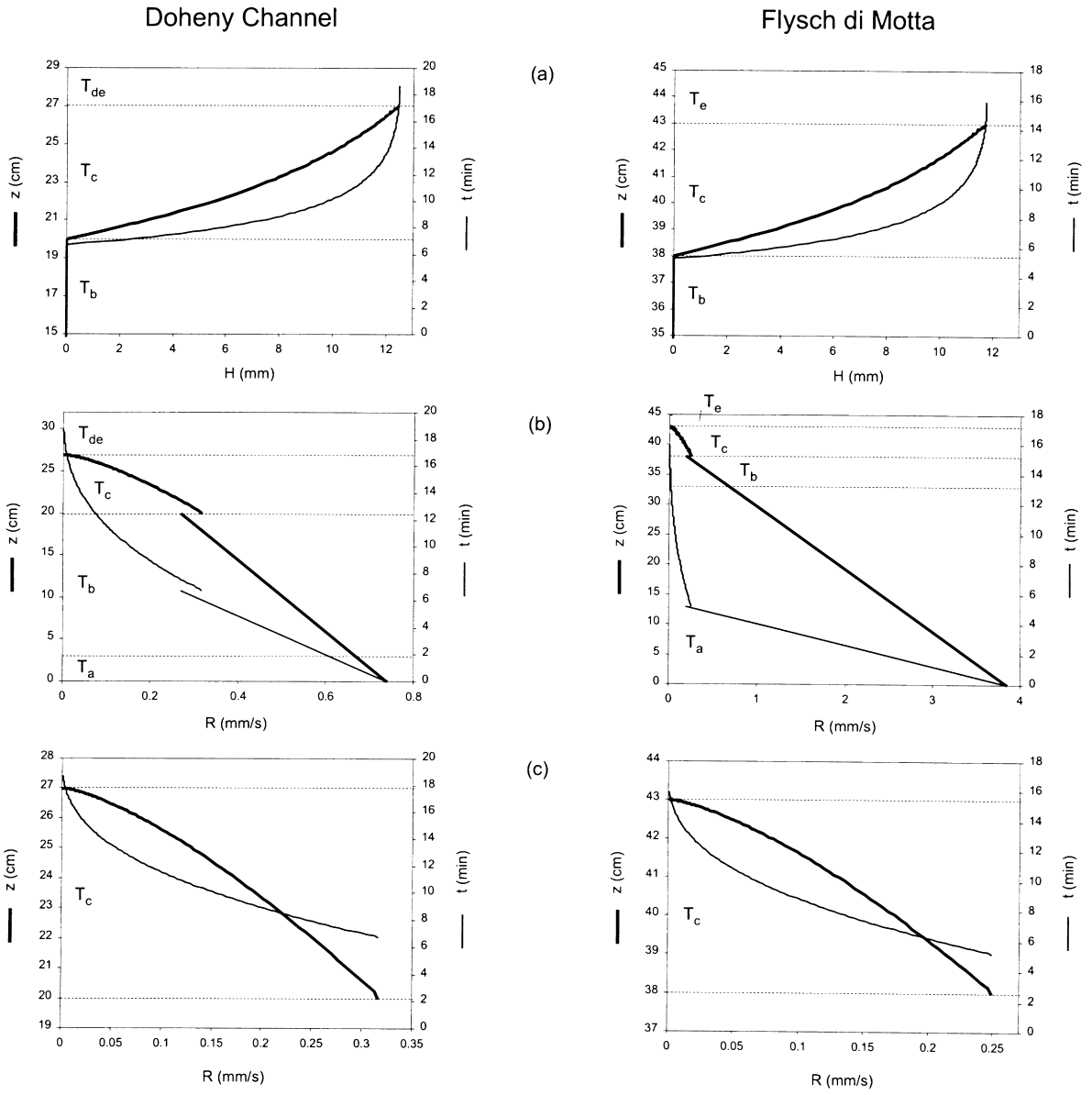

Fig. 5. Calculated spatial (thick lines) and temporal (thin lines) trends in ripple height and sedimentation rate for the Doheny Channel turbidite (left) and bed FM11 from the Flysch di Motta (right). (a) Ripple height development. (b) Sedimentation rate. (c) Enlargement showing sedimentation rate in the T_c-division. The discontinuities in sedimentation rate at the T_{bc}-boundary in (b) are due to the use of different R_{bc}-values in modules 1 and 2 (see text for explanation).

when discussing the test results below. For a total horizontal displacement of the climbing ripples of 32.9 cm and a grain-related mobility parameter decreasing linearly from 0.764 to 0.075 within the limits of the T_c-division, Eq. (17) provides a duration of deposition of 12 min. Combined with the accumulation times for the massive and plane parallel-laminated divisions, T_a and T_b, the total accumulation time for the Doheny Channel turbidite thus adds up to about 19 min (Table 1). This agrees well

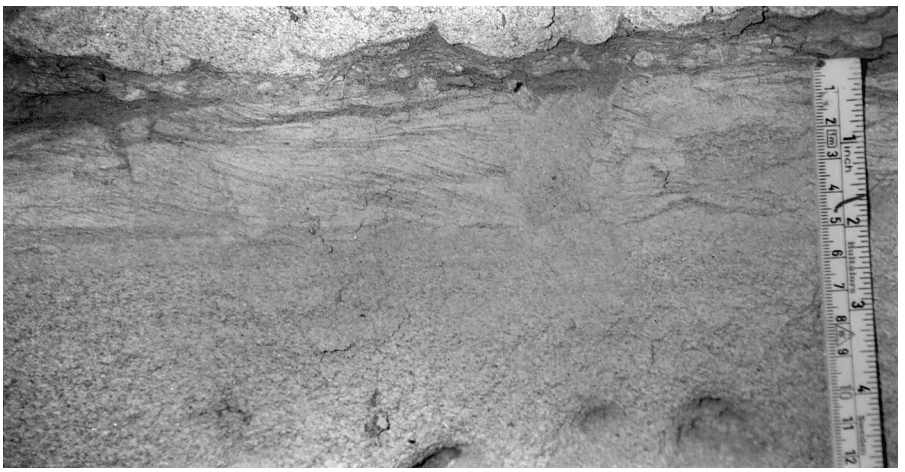

Fig. 6. Upper part of T_a-division, and T_{bce}-divisions in bed FM11. The T_e-division is overlain by a thin turbidite with load casts. Scales on ruler are centimetres (left) and inches (right).

with the lower estimate of 20 min derived by Allen (1991).

Module 3—Fig. 5 summarises temporal and spatial changes in ripple height and sedimentation rate in the Doheny Channel turbidite, calculated with module 3. A rapid increase in ripple height is predicted for the initial stages of development (Fig. 5a). A ripple height of 10 mm is reached within 4 min after the start of rippling. This corresponds to a bed level of about 4.5 cm above the base of the T_c-division. Thereafter, the rate of development decreases until the ripple height is arrested at 12.5 mm at the top of the T_c-division. This agrees well with the observed ripple height of 12 mm. Yet, the theoretical rate of development of ripple height is lower than the observed rate of development, as the main increase in ripple height observed in the Doheny Channel turbidite is confined to the lower 1.5 cm of the T_c-division. It thus appears that TDURE gives an accurate estimate for the final ripple height, but underestimates the development rate towards this height.

By definition, sedimentation rate decreases linearly in the T_a- and T_b-divisions of the Doheny Channel turbidite (Fig. 5b). The gradient in sedimentation rate is non-linear in the T_c-division (Fig. 5c), because of the non-linear decrease in ripple migration rate. The R–t-profile has a concave upward geometry, with the greatest decrease in sedimentation rate occurring in the first 6 min of ripple development. The curve for spatial change in sedimentation rate shows the greatest decrease near the top of the bed (Fig. 5c).

4.2. Flysch di motta

Description—In spite of its misleading name, the Flysch di Motta is a Miocene post-orogenic marine *molasse* succession, exposed on both sides of the Messina Strait, in NE Sicily and SW Calabria, Italy (Fig. 4). The sedimentary succession located south of Reggio di Calabria, between the towns of Lazzaro and Motta San Giovanni, consists of strongly elongated sandstone lobes, composed of stacked and commonly amalgamated sediment-gravity flow deposits, embedded in a heterolithic facies of thinly interlayered fine-grained sandstone and mudstone. The sandstone lobes are 15–54 m thick, 200–700 m wide and possibly up to 20 km long, and have been interpreted as submarine fan lobes derived from contemporaneous deltas (W. Nemec, pers. comm.). The lithofacies within the lobes include thin to moderately thick, medium- to very fine-grained sandstones deposited by high-density turbidity currents (mainly T_{abc}-, T_{ab}-, and T_{ac}-types), and up to 275 cm thick, very coarse- to fine-grained, normally graded and non-graded massive sandstones.

A T_{abce}-bed, exposed along the road from Lazzaro to Motta San Giovanni and hereafter referred to as FM11, was studied in detail for testing TDURE. FM11 has an erosive base. The total bed thickness is

45 cm, of which the T_a-division takes up the largest part with 33 cm. Strings of mud clasts were observed at 20 and 30 cm above the base of the bed. The T_b- and T_c- divisions both have a thickness of 5 cm (Fig. 6). A massive layer of silty mud was found on top of the T_c-division. This interval probably represents the T_e-division. The sampling spacing for grain-size analysis was 5 cm in the T_a-division and 2–3 cm in the other divisions. The sandstone bed is weakly cemented, and gentle crushing sufficed to disintegrate the samples. Dry sieving at a resolution of 0.25ϕ provided detailed grain-size distributions, from which the median size and the sorting coefficient were calculated (Fig. 3b). The turbidite exhibits normal distribution grading from medium to very fine sand (Fig. 3b). According to the classification scheme of Folk (1968), the sorting is moderate to poor. The median grain size at the T_{bc}- and T_{ce}-boundary are 0.135 and 0.076 mm, respectively. The mean ripple height in the T_c-division, based on 11 height measurements, is 12.4 ^ 2.7 mm. Ripples were observed to develop towards this height in the basal centimetre of the T_c-division. The angle of climb of the ripple trains increases from 7° in the lower part, via 9° in the middle part, to 11° in the upper part of the T_c-division.

Module 1—Bed FM11 contains a thicker T_a-division than the Doheny Channel turbidite. Consequently, the sedimentation rate at the base of the bed, obtained by extrapolation of the straight line through the known sedimentation rates at the T_{ab}- and T_{bc}-boundaries to $z = 0$, is considerably larger than in the Doheny Channel turbidite (Table 1). Module 1 provides an accumulation time of 3.02 min for the massive division and 2.21 min for the plane parallel-laminated division. These durations change only slightly (by less than 15 s), when using Eq. (23) instead of Eq. (8).

Module 2—In module 2, the increase in angle of climb from 7° to 11° across the T_c-division was approximated by an average angle of climb of 9°. At this angle, the ripples migrate over a total horizontal distance of 31.6 cm, while the grain-related mobility parameter decreases from 0.780 at the T_{bc}-boundary to 0.085 at the T_{ce}-boundary. The average grain size of 0.101 mm again justifies the use of known empirical relationships between current energy, ripple migration rate and ripple size development for 0.095 mm sand. Module 2 computes an accumulation time of 10.75 min for the T_c-division. Hence, the total duration of deposition for FM11 is almost 16 min (Table 1).

Module 3—The theoretical development of ripple height in FM11 is given in Fig. 5a. As in the Doheny Channel turbidite, ripple height increases most rapidly in the early development stages. According to module 3, the ripples obtain a height of 11.7 mm at $t = \tau_c$. This is indeed close to the observed ripple height, and well within the standard deviation of the measured heights. Bedform stability analysis dictates that ripples of 11–12 mm height should have a linguoid, possibly slightly sinuous plan geometry (Baas, 1994). This is in accordance with the relatively high standard deviation of 2.7 mm and the presence of discontinuous trains of climbing ripples in the turbidite (Fig. 6), both denoting dynamic changes in ripple morphology. As in the Doheny Channel turbidites, TDURE underestimates the rate of development of ripple height. Theoretically, the ripples reach a height of 10 mm at 3.5 cm above the base of the T_c-division. Fig. 6, however, shows that the main increase in height takes place in the lowermost centimetre of that interval. Sedimentation rates follow similar paths as in the Doheny Channel turbidite, but the gradients are different, especially for the T_a- and T_b-divisions (Fig. 5b and c).

5. Discussion

The mathematical equations, on which the duration calculations in TDURE are based, are an inevitable simplification of the natural processes involved in deposition from decelerating high-density turbidity currents. The main assumptions leading to this simplification are the constant temperature of 10°C, the linear decrease in grain-related mobility parameter with time, the constant angle of climb of climbing ripples, and the negligence of suspended sediment fallout in ripple dynamics. The way in which these assumptions affect the model calculations for the Doheny Channel turbidite and the Flysch di Motta turbidite will be discussed below.

The rate of development of current ripples in T_c-divisions is dependent on the local temperature through the viscosity term in the non-dimensional grain parameter, D_* (Eq. (2)). TDURE assumes a

constant temperature of 10°C during turbidite formation. Yet, bottom-water temperatures in many present-day oceans are close to 0°C, while in tropical shelf seas they may be as high as 25°. Moreover, the temperature of a turbidity current may change in time due to mixing with ambient water of contrasting temperature. The standardisation used in TDURE is inevitable however, since in most sedimentary basins ambient and flow temperatures are not known. The temperature dependence of τ_{abc} and $H(\tau_c)$ was tested for the Doheny Channel and Flysch di Motta turbidites using the method of temperature-related hydraulic states (Southard and Boguchwal, 1990). If it were assumed that the turbidites were formed at 0°C instead of 10°C, the 10°C-equivalent ripple height and median grain size would be 18% smaller than the measured values. As a consequence, the total duration of deposition would decrease by about 4 min, and the calculated ripple height would be 1.3 mm and 0.3 mm larger than the measured height for the Doheny Channel turbidite and FM11, respectively. No tests with temperatures higher than 10°C could be conducted, as such tests would involve an increase of equivalent grain size at T_{bc}-boundaries to values for which no u_r–θ'-relationships are available yet (cf. Fig. 1).

The results presented in Table 1 imply that TDURE calculates realistic accumulation times for the studied turbidites, considering the new method used to determine the duration of deposition of the T_c-division. The total duration of deposition agrees well with conservative estimates given by Allen's (1991) original model (e.g. $\tau_{abc} = 20$ min for the Doheny Channel turbidite). These estimates were based on the assumption that traction halts at the top of the T_c-division. The same was assumed in the present study. For both turbidites studied, the accumulation time for the T_c-division, calculated through inferred changes in ripple migration rate (module 2), was shown to predict the final ripple height to within 6% of the observed height, when using empirical equations for ripple growth and a standard temperature of 10°C (module 3). The model is less accurate, however, in predicting the rate of development towards that height. In both examples, the final ripple height was reached at a lower bed height than in the model, so the observed rate of development was greater than the calculated rate. This may be the result of the chosen linear gradient in grain-related mobility parameter across the T_c-division. A more rapid increase in ripple height near the base of the studied beds can be achieved by increasing the time spent in the high-velocity part of the current ripple stability field (cf. Simpson, 1997). In numerical terms, this is equivalent to adopting a power function of the form $\theta' \sim t^m$, with $m > 1$ instead of $m = 1$, as in the linear function. However, even the limiting, unrealistic case that the grain-related mobility parameter remains equal to θ'_{bc} in the entire T_c-division and drops back instantaneously to θ'_{cd} at the top of the bed, does not eliminate the discrepancy between theory and observation. The reason is that the increase in ripple development rate is countered by an increase in sedimentation rate and thus by a decrease in accumulation time. This follows from the fact that an increase in current strength will increase the ripple migration rate, which in turn leads to an increase in sedimentation rate at the constant angle of climb (cf. Eq. (10)). In other words, although the ripples develop at a higher rate, they are given less time to develop. Preliminary tests showed that the thickness of the interval over which the main increase in ripple height takes place cannot be reduced significantly for realistic values of m in the above power function. Other factors should therefore be considered.

One such factor is the constant angle of climb used in the model calculations. A reduction in angle of climb leads to an increase in the duration of deposition for the T_c-division, and a parallel increase in the rate of development of ripple height and final ripple height. Hence, it tends to reduce the discrepancy between theoretical and observed development rate in the studied turbidites, but may introduce dissimilarity between theoretical and observed final ripple height instead. However, the effect of a decrease in angle of climb is limited and insufficient to eliminate the discrepancy in development rate. For example, it was mentioned above that $\xi = 12°$, used in the model calculations for the Doheny Channel turbidite, was identified near the base of the T_c-division (Allen, 1991), and that the angle of climb may be less in the remainder of the bed. Halving the angle of climb to 6° would reduce the bed height at which a ripple height of 10 mm is reached from 4.5 cm to about 2.5 cm, but this is still 1 cm above the observed bed height. At the same angle of climb, module 3 would predict a final ripple height of 13.8 mm, which is unacceptably large

compared to the observed ripple height of 12 mm. In FM11, the thickness of the interval over which main ripple development is inferred to take place reduces by 0.5 cm only, when using an angle of climb of 7° (the lowest angle observed in the bed) instead of 9° in module 3. Again, this is insufficient to explain the observed development rate.

A more fundamental process may be responsible for the discrepancy between observed and calculated development rate. The equations for development of ripple height used in TDURE (Eqs. (4) and (5)) were derived from flume experiments conducted with well-sorted sand and in steady, uniform currents. In such currents, sediment particles that contribute to ripple growth have to be entrained from the bed first. In decelerating turbidity currents, most of these particles are readily available in suspension. The time thus saved may contribute to a greater development rate than accounted for by TDURE, particularly in early stages, when ripples grow quickly and net sedimentation rates are high. Yet, the equilibrium height of the ripples is apparently not affected, considering the above-discussed independence on suspended-load fallout rate (Jopling and Walker, 1968; Walker, 1969; Allen, 1971b; Allen, 1973; Ashley et al., 1982; Arnott and Hand, 1989). In the present model, it is assumed that sediment settling from suspension is distributed evenly over the sediment surface below the turbidity current. This needs to be revised, if the above hypothesis is validated by quantitative data on the development of ripples in the presence of steady fallout of suspended sediment. For now, no such data are available. Finally, the well sorted sand on which Eqs. (4) and (5) are based may be another source for imperfection in the calculation of ripple size development, as turbidites typically consist of moderately to poorly sorted sand. It is unknown, however, how sorting is related to ripple growth.

6. Conclusions

TDURE calculates realistic estimates for the duration of deposition from the decelerating high-density turbidity currents that formed the Doheny Channel turbidite and bed FM11 in the Flysch di Motta. Yet, a thorough evaluation of the model calculations is challenging, since direct observation on the development of Bouma-type sequences below natural and experimental turbidity currents is lacking. Until such data become available, the calculated accumulation times should be regarded as tentative.

TDURE provides accurate measures for the ripple height at the top of the studied turbidite beds. This suggests that the use of empirical equations for ripple dynamics in open channel flows is justified in the analysis of the timing of deposition from turbidity currents. However, since calculations of the rate of development of ripple height are not yet sufficiently accurate, the model would benefit from further testing on a wider range of turbidites.

Acknowledgements

The authors thank Clemens Visser (Delft University of Technology, Netherlands) and Maarten Felix (University of Leeds, UK) for reading an earlier version of the manuscript. The valuable comments of Franco Ricci-Lucchi and an anonymous reviewer are much appreciated. The data from the Flysch di Motta were collected under a research project sponsored by Conoco, Norway.

References

Alexander, L.J.D., 1980. On the geometry of ripples generated by unidirectional open channel flows. Master's thesis, Queens University, Kingston, ON, Canada, 108pp.

Allen, J.R.L., 1971a. Instantaneous sediment deposition rates deduced from climbing-ripple cross-lamination. J. Geol. Soc. Lond. 127, 553–561.

Allen, J.R.L., 1971b. A theoretical and experimental study of climbing-ripple cross-lamination, with a field application to the Uppsala esker. Geogr. Ann. A53, 157–187.

Allen, J.R.L., 1973. Features of cross-stratified units due to random and other changes in bed forms. Sedimentology 20, 189–202.

Allen, J.R.L., 1984. (unabridged one-volume edition). Sedimentary Structures: Their Character and Physical Basis, Elsevier, Amsterdam (pp. 593–663).

Allen, J.R.L., 1991. The Bouma division A and the possible duration of turbidity currents. J. Sediment. Petrol. 61, 291–295.

Arnott, R.W.C., Hand, B.M., 1989. Bedforms, primary structures and grain fabric in the presence of suspended sediment rain. J. Sediment. Petrol. 59, 1062–1069.

Ashley, G.M., Southard, J.B., Boothroyd, J.C., 1982. Deposition of

climbing-ripple beds: a flume simulation. Sedimentology 29, 67–79.

Baas, J.H., 1994. A flume study on the development and equilibrium morphology of small-scale bedforms in very fine sand. Sedimentology 41, 185–209.

Baas, J.H., 1999. An empirical model for the development and equilibrium morphology of current ripples in fine sand. Sedimentology 46, 123–138.

Baas, J.H., de Koning, H., 1995. Washed-out ripples: their equilibrium dimensions, migration rate, and relation to suspended-sediment concentration in very fine sand. J. Sediment. Res. A65, 431–435.

Baas, J.H., Nemec, W., Ravnås, R., Seim, M., 1999. Textural characteristics of deep-marine massive sandstones. 19th Regional European Meeting of Sedimentology, 24–26 August, Geological Institute, University of Copenhagen, Denmark, Abstracts, pp. 22–23.

Bagnold, R.A., 1966. An approach to the sediment transport problem from general physics. US Geological Survey, Professional Paper, 422-I, 37pp.

Bartow, J.A., 1966. Deep submarine channel in Upper Miocene, Orange County, California. J. Sediment. Petrol. 36, 700–705.

Bouma, A.H., 1962. Sedimentology of Some Flysch Deposits: a Graphic Approach to Facies Interpretation, Elsevier, Amsterdam (168pp).

Bowen, A.J., Normark, W.R., Piper, D.J.W., 1984. Modelling of turbidity currents on Navy Submarine Fan, California Continental Borderland. Sedimentology 31, 169–185.

van den Berg, J.H., van Gelder, A., 1993. A new bedform stability diagram, with emphasis on the transition of ripples to plane bed in flows over fine sand and silt. In: Marzo, M., Puigdefabregas, C. (Eds.). Alluvial Sedimentation, International Association of Sedimentologists, pp. 11–21 (Special Publication, 17).

Coleman, S.E., 1991. The mechanics of alluvial stream bed forms, University of Auckland, Department of Civil Engineering, Auckland, New Zealand, Report 517.

Folk, R.L., 1968. Petrology of Sedimentary Rocks, Hemphills, Austin, TX (170pp).

Hiscott, R.N., 1994. Loss of capacity, not competence, as the fundamental process governing deposition from turbidity currents. J. Sediment. Res. A64, 209–214.

Hiscott, R.N., Middleton, G.V., 1979. Depositional mechanics of thick-bedded sandstones at the base of a submarine slope, Tourelle Formation (Lower Ordovician), Quebec, Canada. In: Doyle, L.J., Pilkey, O.H. (Eds.). Geology of Continental Slopes, , pp. 307–326 (SEPM Special Publication, 27).

Jopling, A.V., Walker, R.G., 1968. Morphology and origin of ripple-drift cross-lamination, with examples from the Pleistocene of Masschusetts. J. Sediment. Petrol. 38, 971–984.

Kneller, B.C., Bennett, S.J., McCaffrey, W.D., 1997. Velocity and turbulence structure of density currents and internal solitary waves: potential sediment transport and the formation of wave ripples in deep water. Sediment. Geol. 112, 235–250.

Komar, P.D., 1985. The hydraulic interpretation of turbidites from their grain sizes and sedimentary structures. Sedimentology 32, 395–407.

Kuenen, P.H., 1953. Significant features of graded bedding. AAPG Bull. 37, 1044–1066.

Kuenen, P.H., Migliorini, C.I., 1950. Turbidity currents as a cause of graded bedding. J. Geol. 58, 91–127.

Kühlborn, J.M., 1993. Wachstum und Wanderung von Sedimentriffeln. PhD thesis, Technische Hochschule Darmstadt, Darmstadt, Germany.

Lam Lau, Y., 1985. On the determination of ripple geometry: discussion of Yalin. J. Hydraul. Engng 111, 128–131.

Lowe, D.R., 1982. Sediment gravity flows: II. Depositional models with special reference to the deposits of high-density turbidity currents. J. Sediment. Petrol. 52, 279–297.

Middleton, G.V., 1976. Hydraulic interpretation of sand size distributions. J. Geol. 84, 405–426.

Miller, M.C., McCave, I.N., Komar, P.D., 1977. Threshold of sediment motion under unidirectional currents. Sedimentology 24, 507–527.

Oost, A.P., Baas, J.H., 1994. The development of small scale bedforms in tidal environments: an empirical model and its applications. Sedimentology 41, 883–903.

Piper, D.J.W., Normark, W.R., 1971. Re-examination of a Miocene deep-sea fan and fan-valley, southern California. Bull. Geol. Soc. Am. 82, 1823–1830.

Piper, D.J.W., Shor, A.N., Hughes-Clarke, J.E., 1988. The 1929 “Grand Banks” earthquake, slump, and turbidity current. Geol. Soc. Am., 77–92 (Special Paper 229).

Raudkivi, A.J., 1997. Ripples on stream bed. J. Hydraul. Engng 123, 58–64.

Raudkivi, A.J., Witte, H.H., 1990. Development of bed features. J. Hydraul. Engng 116, 1063–1079.

van Rijn, L.C., 1990. Principles of Fluid Flow and Surface Waves in Rivers, Estuaries, Seas and Oceans, Aqua Publications, Amsterdam (335pp).

van Rijn, L.C., 1993. Principles of Sediment Transport in Rivers, Estuaries and Coastal Seas, Aqua Publications, Amsterdam (700pp).

Rouse, H., 1937. Modern conceptions of the mechanics of turbulence. Trans. Am. Soc. Civil Eng. 102, 436–505.

Seim, M., Baas, J.H., 1999. Vertical trends in grain-size distribution in deep-marine massive sandstones. 19th Regional European Meeting of Sedimentology, 24–26 August, Geological Institute, University of Copenhagen, Denmark, Abstracts, pp. 229–230.

Simpson, J.E., 1997. Gravity Currents in the Environment and the Laboratory, 2nd ed.Cambridge University Press, Cambridge (244pp).

Southard, J.B., Boguchwal, L.A., 1990. Bed configurations in steady unidirectional water flows. Part 2. Synthesis of flume data. J. Sediment. Petrol. 60, 658–679.

Stow, D.A.V., Bowen, A.J., 1978. Origin of lamination in deep-sea, fine-grained sediments. Nature 274, 324–328.

Stow, D.A.V., Bowen, A.J., 1980. A physical model for the transport and sorting of fine-grained sediment by turbidity currents. Sedimentology 27, 31–46.

Storms, J.E.A., van Dam, R.L., Leclair, S.F., 1999. Preservation of cross-sets due to migration of current ripples over aggrading and non-aggrading beds: comparison of experimental data with theory. Sedimentology 46, 189–200.

van Tassell, J., 1981. Silver abyssal plain carbonate turbidite: flow characteristics. J. Geol. 89, 317–333.

Tsujimoto, T., Nakagawa, H., 1982. Sand wave formation due to irregular bed load motion. In: Mutlu Sumer, B., Müller, A. (Eds.), Mechanics of Sediment Transport. Proceedings of Euromech, 156, pp. 109–117.

Walker, R.G., 1969. Geometrical analysis of ripple-drift cross-lamination. Can. J. Earth Sci. 6, 383–391.